

Infrared Studies of Carbon Monoxide Hydrogenation over Alumina-Supported Ruthenium

C. STEPHEN KELLNER AND ALEXIS T. BELL

Materials and Molecular Research Division, Lawrence Berkeley Laboratory, and Department of Chemical Engineering, University of California, Berkeley, California 94720

Received February 12, 1981; revised June 2, 1981

The nature of the species present on a Ru/Al₂O₃ catalyst during CO hydrogenation was studied by means of Fourier-transform infrared spectroscopy. Three forms of adsorbed CO were identified, designated as linearly adsorbed, diadsorbed, and μ -bridge adsorbed. The coverage by the linearly adsorbed form of CO obeys a Langmuir isotherm under reaction conditions. The equilibrium constant associated with this isotherm is given by $K_{CO} = 1.1 \times 10^{-9} \exp(25,000/RT) \text{ atm}^{-1}$. The diadsorbed species is associated with individual Ru atoms and clusters and, in contrast to linearly adsorbed CO, does not readily undergo hydrogenation at temperatures below 548 K. The μ -bridge form of adsorbed CO may involve either a pair of Ru sites or a Ru site and an adjacent Lewis acid site. Hydrocarbon, formate, and carbonate structures were also observed in the course of this study. It was established, however, that these species are present on the alumina support and are not intermediates of CO hydrogenation over Ru.

INTRODUCTION

Infrared spectra taken during the hydrogenation of CO over ruthenium catalysts have helped to identify the dominant species adsorbed on the catalyst (1-5). Dalla Betta and Shelef (1) have reported that the surface of a Ru/Al₂O₃ catalyst is nearly saturated by adsorbed CO at temperatures up to 523 K. It was suggested that the presence of hydrogen on the catalyst surface weakens the C-O bond of chemisorbed CO, since the band for this species appeared at a lower frequency than that observed for CO chemisorbed in the absence of hydrogen. At higher temperatures the buildup of carbon on the catalyst caused a further shift of the CO bond to lower frequencies and a decrease in the band intensity. Bands attributable to hydrocarbon, formate, and carbonate structures were also observed but these species were ascribed to reaction products adsorbed on the support. Chemisorbed CO has also been observed as a dominant species in the studies conducted by Ekerdt and Bell (2, 3) using a Ru/SiO₂ catalyst. In this work the position and intensity of the CO band were found to be independent of the H₂/CO ratio

or the CO partial pressure. A decrease in the band intensity, unaccompanied by a shift in position, was observed with increasing temperature and was ascribed to a reduction in the CO coverage. Bands were also observed for hydrocarbon species. These structures could be removed from the catalyst surface by hydrogenation, but did not appear to be intermediates in the synthesis of stable products. Additional observations concerning the hydrocarbon structures formed on Ru/SiO₂ and Ru/Al₂O₃ catalysts have been presented by King (4, 5). Strong bands attributable to long-chain saturated hydrocarbons were observed at temperatures below 473 K. While the exact point of attachment of these structures could not be defined, it was concluded that the species observed were not intermediates in the formation of gas-phase products. At higher temperatures changes in the shape and position of the hydrocarbon band suggested the presence of short-chain species. It was proposed that these species are attached to the metal surface and might be intermediates in the synthesis reaction.

The primary objective of the present investigation was to characterize more fully

the influence of reaction conditions on the concentration of the species absorbed on a Ru/Al₂O₃ catalyst during CO hydrogenation. Fourier-transform infrared spectroscopy was used for this purpose, and particular attention was devoted to interpretation of the bands ascribed to chemisorbed CO. Working under conditions chosen to avoid significant catalyst deactivation, three different forms of absorbed CO were identified. These are designated as linearly absorbed, diabsorbed, and μ -bridge-absorbed CO. A detailed study was made of the effects of reaction conditions on the position and intensity of the band associated with the linearly absorbed CO. On the basis of these observations, estimates were made of the variation in the coverage by this species with CO partial pressure and catalyst temperature. As a complement to these studies the kinetics of forming C₁ through C₁₀ hydrocarbons were examined in detail. The results of these efforts together with a discussion of the mechanism of hydrocarbon synthesis over ruthenium is presented separately (6).

EXPERIMENTAL

The 1% Ru/Al₂O₃ catalyst used for these studies was prepared by absorption of the Ru₆C(CO)₁₇ from pentane solution onto Kaiser KA-201 alumina. Details concerning synthesis of the complex, impregnation of the support, and the reduction of the final catalyst are described in Refs. (6, 7). A 75-mg portion of the reduced catalyst was pressed into a 20 × 0.25-mm disk and placed inside a small infrared reactor (8). The dispersion of the freshly prepared catalyst, determined by H₂ chemisorption, was ~1.0.

Prior to each series of experiments, the catalyst was reduced in flowing H₂ for 10 to 12 hr at 673 K and 10 atm. The temperature was then lowered to 498 K and a premixed feed, containing H₂ and CO, was introduced at a flow rate of 200 cm³/min (NTP). Ten minutes after reaction had begun, the effluent gas was analyzed by gas chroma-

tography (6), and the gas feed was switched over to pure H₂ for 1 hr. By alternating short reaction periods and longer reduction periods, a stable catalyst activity could be achieved after several cycles. The Ru dispersion decreased to 0.52 during the initial reaction periods but remained constant thereafter. Once a stable catalyst activity had been obtained, reaction conditions were adjusted to those desired for a particular experiment. For all of the conditions used in the present study, methane, C₂ through C₁₀ hydrocarbons (mainly olefins), and methanol were observed as the primary synthesis products (6).

Infrared spectra were taken with a Digilab FTS-10M Fourier-transform infrared spectrometer, using a resolution of 4 cm⁻¹. For the observation of steady-state phenomena, 100 interferograms, each acquired in about 1.25 s, were co-added to improve the signal-to-noise ratio. However, good spectra could also be obtained by co-adding as few as 10 interferograms. In addition to recording spectra of the catalyst under reaction conditions, spectra were also recorded of the catalyst, following reduction in H₂, and of a support disk, placed downstream from a catalyst disk, during reaction. The latter two spectra were used to subtract out infrared absorptions due to the support and the gas phase.

RESULTS AND DISCUSSION

Infrared spectra of the catalyst taken under reaction conditions showed bands in two regions, one set appearing between 3200 and 2700 cm⁻¹ and another set appearing between 2300 and 1200 cm⁻¹. The bands in the first of these regions are associated with absorbed hydrocarbons, while bands in the second region are due to carbonyl, carbonate, and formate structures. To identify whether these structures are present on the surface of the metal and/or support and to identify the relative stability and reactivity of individual structures, spectra were taken under a variety of conditions.

Bands Observed between 2300 and 1200 cm^{-1}

Spectral observations. Representative spectra of the most prominent features observed in this region, during reaction at pressures of 1, 5, and 10 atm, are shown in Fig. 1a. The spectrum shown at each pressure represents the difference in the absorbances of the catalyst and reference disks, measured in the presence of the same gas composition. A broad band can be seen near 2000 cm^{-1} superimposed on which is a weakly defined shoulder of 2040 cm^{-1} and a partially resolved band at 1960 cm^{-1} . All three features appear immediately upon passage of the H_2 -CO mixture over the catalyst and the integrated intensity of the band envelope grows by about 10–15% over a 20-min period of observation. It is significant to note, though, that the positions of the three bands are totally unaltered during this period. Figure 1b shows spectra taken following cessation of the reaction and reduction in H_2 . The intense band near 2000 cm^{-1} is now completely eliminated, thereby revealing very clearly the bands at 2040 and 1960 cm^{-1} . It is noted that the intensities of these two peaks are independent of the reaction pressure. Moreover, the structures giving rise to these features are stable to reduction at

temperatures below 548 K and can only be removed at higher temperatures. Spectra of the species removed by reduction at reaction temperatures are shown in Fig. 1c, and are obtained by taking the difference between the spectra presented in Figs. 1a and b. Each spectrum consists of a broad, asymmetric band which does not return to the baseline at low frequencies. With increasing reaction pressure, the intensity of this band increases and the band maximum shifts to higher frequencies.

The effects of temperature on the spectra of the species susceptible to H_2 reduction are illustrated in Fig. 2. The spectra shown in this figure represent the difference between spectra taken under reaction conditions and those obtained following H_2 reduction of the catalyst at the reaction temperature. This mode of presentation is similar to that used in Fig. 1c, with the exception that bands associated with the gas phase and species weakly bound to the support are not subtracted out. The series of peaks occurring between 2300 and 2060 cm^{-1} is due to gas-phase CO. These bands are clearly evident in spectrum e, which was obtained under the conditions of spectrum b using a disk of alumina free of Ru. Both the position and intensity of the band near 2000 cm^{-1} depend on the catalyst temperature. As the temperature increases, the band maximum shifts to lower frequencies and the intensity decreases.

In addition to the major features appearing at 2000 cm^{-1} , a broad band can be seen in Fig. 2, which extends between 1800 and 1200 cm^{-1} . Superimposed on this band are five more sharply defined bands at 1750, 1590, 1450, 1390, and 1370 cm^{-1} . Only the weak band at 1750 cm^{-1} is due to chemisorbed CO. On the basis of studies by Dalla Betta and Shelef (1) and King (4, 5), the bands at 1590, 1390, and 1370 cm^{-1} can be assigned to formate structures, and the band at 1450 cm^{-1} can be assigned to carbonate structures. Both types of species are formed on the alumina support and accumulate during reaction. Upon reduction of

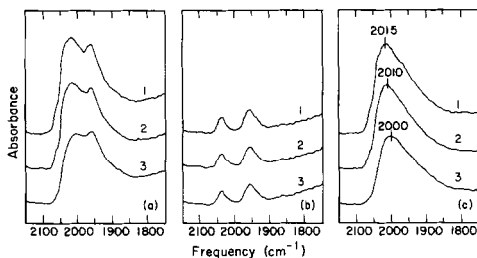


FIG. 1. Spectra obtained at 458 K during reaction and subsequent reduction in H_2 : (a1) $P = 10 \text{ atm}$, $\text{H}_2/\text{CO} = 2$; (a2) $P = 5 \text{ atm}$, $\text{H}_2/\text{CO} = 2$; (a3) $P = 1 \text{ atm}$, $\text{H}_2/\text{CO} = 2$; (b1) after (a1) and following reduction in H_2 at 10 atm; (b2) after (a2) and following reduction in H_2 at 5 atm; (b3) after (a3) and following reduction in H_2 at 1 atm; (c1) difference between (a1) and (b1); (c2) difference between (a2) and (b2); (c3) difference between (a3) and (b3).

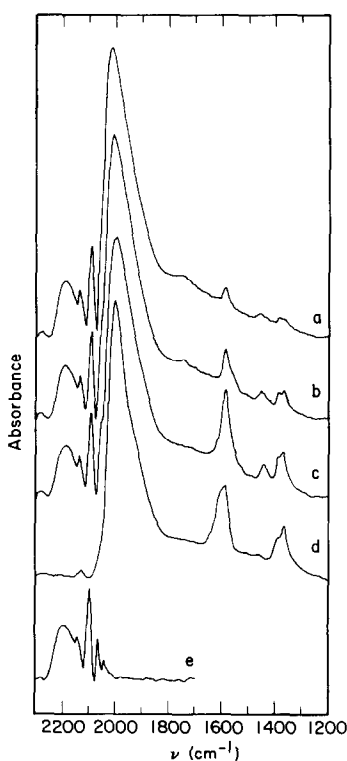


FIG. 2. Spectra of chemisorbed CO under reaction conditions and following adsorption of CO: (a) sample spectrum— $H_2/CO = 2$, $P = 1$ atm, $T = 498$ K; reference spectrum—after reduction in H_2 at 1 atm and 498 K; (b) sample spectrum— $H_2/CO = 2$, $P = 1$ atm, $T = 523$ K; reference spectrum—after reduction in H_2 at 1 atm and 523 K; (c) sample spectrum— $H_2/CO = 2$, $P = 1$ atm, $T = 548$ K; reference spectrum—after reduction in H_2 at 1 atm and 548 K; (d) sample spectrum—after CO adsorption at 1 atm and 523 K and elution of gas-phase CO with He; reference spectrum—after reduction in H_2 at 1 atm and 523 K; (e) sample spectrum— $P_{CO} = 1$ atm, $T = 523$ K; reference spectrum—after reduction in H_2 at 1 atm and 523 K.

the catalyst in H_2 , the intensity of the bands associated with these species diminishes. As a result, the background spectra used in obtaining the spectra presented in Fig. 2 show a decrease in the intensity of the formate and carbonate bands with increasing temperature, and, consequently these bands are emphasized in the difference spectra shown.

The similarity of spectra obtained under reaction conditions with those obtained by exposure of the catalyst to CO alone can be

seen by comparison of spectra b and d in Fig. 2. The latter spectrum was obtained after passing CO over the catalyst for 5 min and then eluting the gaseous CO with He for 0.5 min. With the exception of the gas-phase bands, which are not present in spectrum d, spectra b and d are virtually identical.

A more detailed illustration of features appearing on the low-frequency side of the principal carbonyl band is shown in Fig. 3. This spectrum is similar to spectrum d in Fig. 2 but was obtained at 448 K. At this temperature the formate and carbonate structures are not removed upon reduction and consequently the bands associated with these species are subtracted out completely. The broad band between 1800 and 1200 cm^{-1} is now seen to be composed of two broad bands centered at approximately 1700 and 1500 cm^{-1} . In addition, a definite shoulder can be observed at 1920 cm^{-1} , on the low-frequency side of the band near 2000 cm^{-1} .

All of the bands observed in Figs. 1 and 2 are attenuated slowly upon passage of He over the catalyst and much more rapidly in the presence of H_2 . An illustration of these changes is shown in Fig. 4. Passage of He over the catalyst causes a slow decrease in the intensity of the principal band and a concurrent downscale shift in its position. More careful examination of spectra 1 through 4 reveals that initially intensity is lost from the high-frequency portion of the principal absorption band and from the

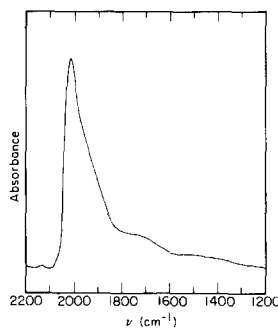


FIG. 3. Spectrum obtained following CO adsorption at 1 atm and 448 K and elution of gaseous CO by He.

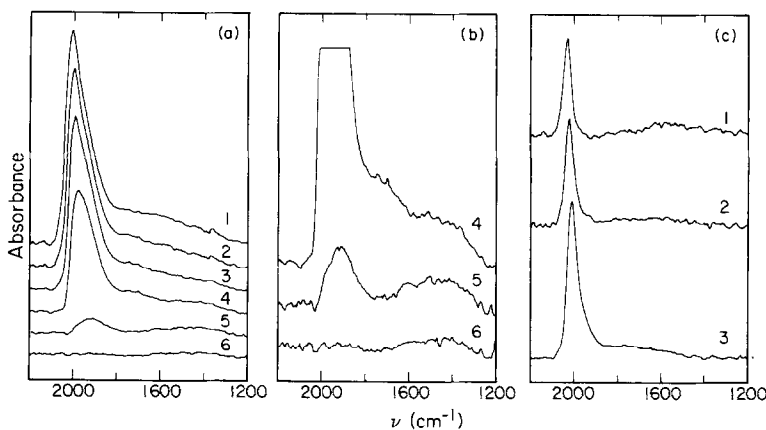


FIG. 4. Effects of He and H₂ on the intensities of bands associated with adsorbed CO: adsorption conditions— $P_{\text{CO}} = 3.3$ atm, $T = 498$ K; (a1) following exposure to a He flow at 498 K for 0.5 min; (a2) 2.7 min; (a3) 14.0 min; (a4) 46.0 min; (a5) following exposure to a H₂ flow at 498 K for 0.2 min; (a6) 0.5 min; (b4) same as (a4) expanded fourfold; (b5) same as (a5) expanded fourfold; (b6) same as (a6) expanded fourfold; (c1) difference between (a1) and (a2) expanded twofold; (c2) difference between (a2) and (a3) expanded twofold; (c3) difference between (a3) and (a4) expanded twofold.

peaks present below 1900 cm^{-1} . This observation is supported by spectrum 1 in Fig. 4c, which represents the difference between spectra 1 and 2 in Fig. 4a. With increasing time, the region from which intensity is lost shifts toward lower frequencies, indicating that the position of the high-frequency component of the principal band shifts to lower frequencies as its intensity decreases. Eventually, though, intensity is lost from both the high- and low-frequency regions of the principal absorption band and from the peak located near 1700 cm^{-1} . Spectra 2 and 3 in Fig. 4c illustrate these changes.

The relationship between the position of the principal band and the relative integrated absorbance of the band is shown in Fig. 5. If it is assumed that the extinction coefficient associated with this band is constant, then the abscissa in this figure is equivalent to a fractional surface coverage. The plot is seen to consist of two distinct branches. As the ratio A/A_s decreases from unity, ν_{CO} shifts from 2030 cm^{-1} to lower values but at an ever decreasing rate. When A/A_s reaches 0.55, the decrease in ν_{CO} accelerates. Finally, at $A/A_s = 0.2$, ν_{CO} reaches a value of 1950 cm^{-1} .

Figure 4 also shows that the reduction of preadsorbed CO in H₂ causes a very rapid decline in the intensity of the high-frequency side of the principal band and of the broad band centered at 1700 cm^{-1} . As a consequence, the bands located at 1920 and 1500 cm^{-1} can now be seen more clearly. Spectrum 4 in Fig. 4b shows that the bands are also attenuated as the duration of reduction is extended.

Assignment of carbonyl bands. The present results show that as many as six bands can be identified for chemisorbed

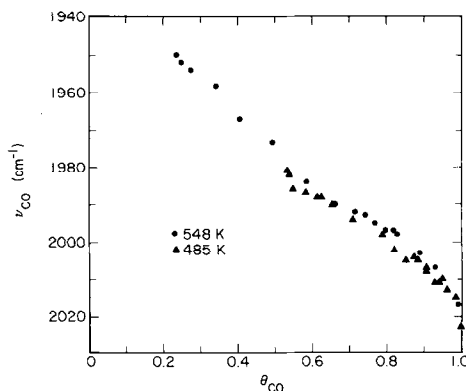


FIG. 5. Relationship between the frequency of the principal carbonyl adsorption band and the coverage by linearly adsorbed CO.

CO, located at 2040, 2030–1950, 1920, 1750, 1700, and 1500 cm^{-1} . The assignment of these features to specific structures is examined next, following which the stability and reactivity of the various forms of adsorbed CO are discussed.

The strong band observed between 2030 and 1950 cm^{-1} falls within the range of frequencies (2085 to 1950 cm^{-1}) associated with linearly bonded CO in Ru carbonyl complexes (9). As a result, it is reasonable to assign this band to linearly adsorbed CO. This interpretation is further supported by recent EELS (10) and reflectance infrared (11) studies of CO adsorbed on a Ru(001) surface. The spectra obtained in these investigations exhibit a single band which shifts with increasing CO coverage from about 1980 cm^{-1} to as high as 2080 cm^{-1} , as a result of strong lateral interactions in the adlayer. LEED (10, 12–14) and ESDIAD (15) observations support the assignment of this band to linearly adsorbed CO.

While the shift in band position with coverage observed in the present work is of the same magnitude as that reported for CO adsorption on Ru(001) surfaces (10, 11), the highest and lowest frequencies observed in the single-crystal studies are notably higher than those shown in Fig. 5. This difference may be due to differences between the physical properties of alumina-supported Ru microcrystallites and bulk Ru metal. It is also possible that at least a part of the difference may be due to the presence of carbon on the surface of the supported Ru, formed by CO disproportionation. Carbon has been found to act as an electron donor and to enhance the back-donation of electronic charge from the metal to the π^* orbitals of CO (1). This would have the effect of weakening the C–O bond and shifting its frequency downscale. It is significant to note, that while carbon deposition via CO disproportionation has been observed for alumina-supported Ru (16, 17), no evidence has been reported for the occurrence of this reaction on Ru(100), (001), (101), (110) surfaces studied at low pressures (12, 18–21).

As was noted earlier, during reaction the band near 2000 cm^{-1} undergoes a moderate (10–15%) growth in intensity which is unaccompanied by changes in the band position. A possible explanation for this observation is that the Ru dispersion increases slightly with time of reaction but that the fractional coverage of the surface remains the same. The fact that such changes are not observed upon exposure of the catalyst to CO alone and that the rate of change is accelerated by higher reaction pressure, at a fixed H_2/CO ratio and temperature, suggests that the changes in Ru dispersion may be caused by the local release of the heat of CO hydrogenation. Under this influence some of the smaller three-dimensional microcrystallites may be converted to two-dimensional rafts, thereby exposing a greater fraction of surface Ru atoms.

The spectra presented in Figs. 1 and 2 indicate that both the frequency and intensity of the band assigned to linearly adsorbed CO decrease with decreasing CO partial pressure and increasing catalyst temperature. Since, as was shown in Fig. 3, the spectra observed for CO chemisorbed in the presence and absence of H_2 are virtually identical, it seems reasonable to propose that the changes observed under reaction conditions can be ascribed to changes in the coverage of the Ru surface by linearly adsorbed CO. Because of the increase in band intensity with duration of reaction, discussed above, band intensity cannot be used as a reliable measure of the coverage of linearly bonded CO. An estimate of the fraction of the total sites which could be covered at saturation by this species can be attained, however, by assuming that the extinction coefficient for the band near 2000 cm^{-1} is independent of coverage and then using the relationship between frequency and coverage noted in Fig. 5. It should be noted, though, that the assumption underlying such calculations is not fully established. In studies conducted by Pfnür *et al.* (11), the intensity of the infrared band associated with CO chemisorbed on a Ru(001) surface was found to increase lin-

early with CO coverages, up to a coverage of one-half of saturation. For higher coverages, the integrated intensity declined. These results would suggest that the extinction coefficient decreases at coverages approaching saturation. However, since only a monotonic change in integrated intensity with coverage was observed in the present work, it can be concluded that the trend observed for a Ru(001) surface does not necessarily apply to alumina-supported Ru microcrystallites.

Applying the approach described above, a series of isotherms can be constructed to determine the coverage of linearly adsorbed CO under reaction conditions. Figure 6 shows that on a plot of θ_{CO}^{-1} versus P_{CO}^{-1} the data fall along straight lines, independent of the H_2 partial pressure. Consequently, θ_{CO} can be described by a Langmuir isotherm of the form

$$\theta_{\text{CO}} = \frac{K_{\text{CO}}P_{\text{CO}}}{1 + K_{\text{CO}}P_{\text{CO}}}, \quad (1)$$

where K_{CO} is the effective equilibrium constant for CO adsorption. From the slopes of the lines presented in Fig. 6 it is determined that

$$K_{\text{CO}} = 1.1 \times 10^{-9} \exp(25,500/RT) \text{ atm}^{-1}. \quad (2)$$

The heat of adsorption appearing in Eq. (2) is in excellent agreement with activation energies for CO desorption determined in

studies conducted with Ru single crystals (17-21) and, in particular, with the value reported by Pfnür *et al.* (21) for desorption from Ru(001) at near-saturation coverage. The present results also agree with the activation energy for CO desorption determined for the weaker of the two adstates reported by Low and Bell (22) for Ru/ Al_2O_3 . The stronger state is characterized by an activation energy of 37 kcal/mole and, hence, would be fully saturated at the high CO coverages reported here. The preexponential factor in Eq. (2) is two orders of magnitude smaller than that calculated from data presented by Pfnür *et al.* (21). A possible explanation for this difference may be that the frequency factor for CO desorption from the surface of alumina-supported Ru is two orders of magnitude higher than that for desorption from a Ru(001) surface.

The observations concerning the band for linearly adsorbed CO reported here are in qualitative agreement with previous studies of a similar nature, but some differences exist with regard to the interpretation of the shifts in band position with reaction conditions. Working with a 5% Ru/ Al_2O_3 catalyst, Dalla Betta and Shelef (1) reported that the spectrum of CO adsorbed at 523 K from a 1-atm CO/He mixture (0.025:0.975 mole fraction) exhibited a single band centered at 2043 cm^{-1} . When the catalyst was contacted with a H_2 /CO/He mixture (0.075:0.025:0.900) at the same temperature and pressure, the band shifted to 1996 cm^{-1} , and the integrated band intensity decreased by 12%. A similar effect of H_2 was noted by King (4) in studies performed with a 1% Ru/ Al_2O_3 catalyst. Dosing the catalyst with CO at room temperature produced a band at 2045 cm^{-1} which shifted to 2020 cm^{-1} following exposure of the adsorbed CO to a H_2 pressure of 5.4 atm. Both Dalla Betta and Shelef (1) and King (4) have proposed that the shift in CO frequency could be attributed to an increase in the availability of electrons for back-bonding from the metal to the adsorbed CO, resulting from the presence of

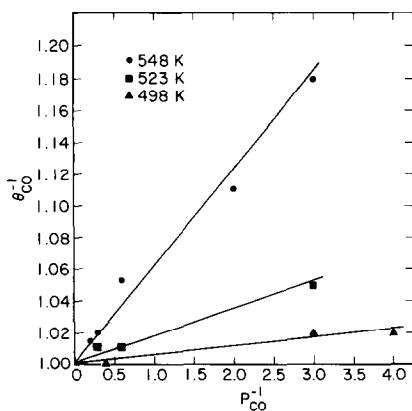


FIG. 6. Relationship between θ_{CO}^{-1} and P_{CO}^{-1} during reaction.

coadsorbed H atoms. While this interpretation is plausible, it seems that one could equally well explain these observations in terms of a decrease in the dipole-dipole interactions resulting from a small change in the surface coverage by CO (11). As may be seen in Fig. 5, a 15% decrease in the integrated absorbance of the band from its maximum value corresponds to a shift in the band from 2030 to 2000 cm^{-1} . Selection between these two interpretations is not clear-cut, particularly since the influence of adsorbed hydrogen may be affected by the partial pressures of H_2 and CO used for specific experiments.

Dalla Betta and Shelef (1) and King (4) reported that increasing the temperature while passing a continuous flow of H_2 and CO over the catalyst caused a downscale shift in the position of the band for linearly adsorbed CO and a reduction in the band intensity. Provided temperatures did not exceed ~ 523 K and reaction times were relatively short, the initial CO band could be restored simply by cooling the catalyst in the flowing H_2/CO mixture. At higher temperatures and with durations of reaction exceeding several hours, much of the CO band intensity remained lost upon cooling. Dalla Betta and Shelef (1) attributed the irreversible changes in CO band position and intensity to the interaction of the metal with a carbonaceous deposit. King (4) concurs with this explanation but suggests that the reversible changes in the band characteristics are due to depletion via reaction of more weakly bound forms of CO which exhibit absorptions toward the high-frequency side of the CO band.

In the present study the duration of reaction was kept to less than 20 min and the temperature never exceeded 548 K, in order to avoid extensive catalyst deactivation due to the buildup of carbon. As a result, it is believed that the changes in CO band frequency and intensity with temperature shown in Fig. 2 are not due to the accumulation of carbon on the catalyst surface but, rather, to changes in the coverage of linearly adsorbed CO.

The bands observed at 2040 and 1960 cm^{-1} in the present work are very similar to those reported by Kuznetsov *et al.* (7) in their studies of the structures formed upon decomposition of alumina-supported $\text{Ru}_3(\text{CO})_{12}$, $\alpha\text{-H}_4\text{Ru}_4(\text{CO})_{12}$, and $\text{Ru}_6\text{C}(\text{CO})_{17}$. In each case, reduction of the supported cluster in H_2 at temperatures less than 573 K led to the appearance of two bands of nearly comparable intensity, located at 2047–2052 and 1965–1970 cm^{-1} . Comparison of the positions of these bands with those for Ru-halocarbonyl complexes leads to the conclusion that the two bands arise from structures of the form $[\text{Ru}(\text{CO})_2\text{X}_2]_n$ (7, 9). The element X in this structure is assumed to be the oxygen of the alumina lattice and the number n represents the number of Ru atoms present in the surface structure.

Consistent with the proposed interpretation, the bands appearing at 2040 and 1960 cm^{-1} can be associated with the symmetric and asymmetric modes of vibration of C–O bonds in a pair of CO molecules attached to a common Ru site. The angle between the two CO molecules, 2α , can be estimated from the ratio of the integrated absorbances of the symmetric and asymmetric bands, A_{sym} and A_{asym} , by means of Eq. (3) (23–25):

$$A_{\text{asym}}/A_{\text{sym}} = \tan^2\alpha. \quad (3)$$

This relationship has been shown to provide an accurate measure of α for dicarbonyl transition metal complexes in which the two CO ligands are in a *cis* configuration. Application of Eq. (3) to the bands at 1960 and 2040 cm^{-1} leads to an estimate of $100 \pm 5^\circ$ for the angle between the two CO molecules attached to a common Ru site. By way of comparison, it is noted that bond angles between 93 and 96° have been reported for $(\pi\text{-C}_5\text{H}_5)\text{Fe}(\text{CO})_2\text{X}$ ($\text{X} = \text{Cl}, \text{Br}, \text{I}$) and a bond angle of 91° has been reported for $\text{Rh}_2(\text{CO})_4\text{Cl}_2$ (24, 26). Thus, it appears that the angle between diadsorbed CO molecules is similar to that found for transition metal complexes.

The independence of the vibrational frequencies associated with the diadsorbed CO structures on the coverage by singly adsorbed CO indicates that the two structures are, most likely, not coupled by dipole-dipole interactions (25). This observation together with the fact that the diadsorbed CO is much more stable to decomposition or reduction than monoadsorbed CO, suggests that the diadsorbed structures occur at sites isolated from the Ru crystallites. Examples of such sites might be individual Ru atoms or small Ru clusters. This interpretation is supported by the fact that the intensity of the bands at 2040 and 1960 cm^{-1} can be attenuated significantly by extended exposure of the catalyst to CO without affecting the intensities or positions of other CO bands (27).

The band appearing at 1920 cm^{-1} in Fig. 3 occurs at a frequency about 30 cm^{-1} lower than that normally ascribed to linearly bonded CO in unsubstituted Ru carbonyls. However, C-O vibrational frequencies as low as 1900 cm^{-1} have been observed for linearly bonded CO in Ru carbonyl complexes containing nucleophilic ligands (9). In view of this, the band at 1920 cm^{-1} can be assigned to CO adsorbed in a linear mode at a site adjacent to a nucleophilic adsorbate. The most likely candidate for the latter species is carbon, formed as an intermediate in either CO disproportionation or hydrogenation.

The weak peak at 1750 cm^{-1} and the broad peaks at 1700 and 1500 cm^{-1} appear at frequencies much lower than those normally associated with bridging carbonyls (1880–1813 cm^{-1}) in Ru complexes (9). Recent studies have shown that CO vibrations do occur in this portion of the spectrum for μ -bonded carbonyls, in which coordination occurs through both the carbon and oxygen atoms of CO, and for adducts formed between metal carbonyls and Lewis acids. When coordination takes place exclusively with metal atoms, CO frequencies of 1645 cm^{-1} for $\text{Mn}_2(\text{CO})_5(\text{Ph}_2\text{PCH}_2\text{PPh}_2)_2$ (28) and 1330 cm^{-1} for $(\eta^5\text{-C}_5\text{H}_5)_3\text{Nb}_3(\text{CO})_7$ (29) have

been observed. The large difference in these frequencies reflects the fact that μ -bonding can occur in different ways. In the case of adducts of metal carbonyls with Lewis acids, C-O stretching frequencies are observed in the range of 1530–1700 cm^{-1} (19, 30). In the case of $\text{Ru}_3(\text{CO})_{12} \cdot \text{AlBr}_3$, a strong band is seen at 1535 cm^{-1} and spectra of the 1:1 and 1:2 adducts of $[(\pi\text{-C}_5\text{H}_5)\text{Ru}(\text{CO})_2]_2$ with isobutyl aluminum exhibit a band at 1680 cm^{-1} (9, 30).

Reactivity of carbonyl structures. The spectra presented in Figs. 1 and 3 demonstrate that the different forms of adsorbed CO exhibit significant differences in reactivity with respect to H_2 . The two types of linearly adsorbed CO, which are characterized by the band appearing between 2030 and 1950 cm^{-1} and the band appearing at 1920 cm^{-1} , react rapidly with H_2 . Transient-response experiments (31) have shown that the dynamics of the disappearance of these bands correlate closely with the formation of methane and water, which suggests that linearly adsorbed CO is the primary source of carbon for the synthesis reaction. Figure 3 shows that the band at 1700 cm^{-1} is also attenuated rapidly during H_2 reduction. No study has been made of the reaction dynamics associated with this band and hence it is not possible to conclude whether the μ -bonded form of CO which this band represents is an important reaction precursor.

The pair of bands at 2040 and 1960 cm^{-1} are relatively stable to reduction and attenuate only slowly at temperatures above 300°C. This fact, plus the general behavior of these bands, suggests that diadsorbed CO does not enter into the synthesis of hydrocarbons under the reaction conditions examined in these studies. Consistent with this conclusion it has been found (27) that catalysts which exhibit a high proportion of diadsorbed CO relative to singly adsorbed CO are less active than catalysts which exhibit the reverse relationship between the two forms of adsorbed CO. The μ -bonded form of CO characterized by the band at

1500 cm^{-1} is only slightly less reactive than the linearly adsorbed form of CO. However, because of the weak intensity of this band it has not been possible to relate the intensity of this band to the catalyst activity.

Bands Observed between 3200 and 2700 cm^{-1}

Figure 7 shows a sequence of spectra for the frequency range between 3200 and 2400 cm^{-1} , taken at different times during the course of a run. The spectrum taken after 0.5 min shows only a very noisy baseline due to the poor transmission of the catalyst disk in this frequency regime. After 10 min of reaction, well-defined peaks can be detected at 2930 and 2860 cm^{-1} . The intensity of these features increase steadily with time and after 20 min a shoulder can be detected at 2960 cm^{-1} in addition to the two more intense bands. It is significant to note that over the same period of time the intensity of the principal CO band increases by less than 8% and its position remains fixed at 2010 cm^{-1} .

Spectra of the C-H stretching region taken at different temperatures, pressures,

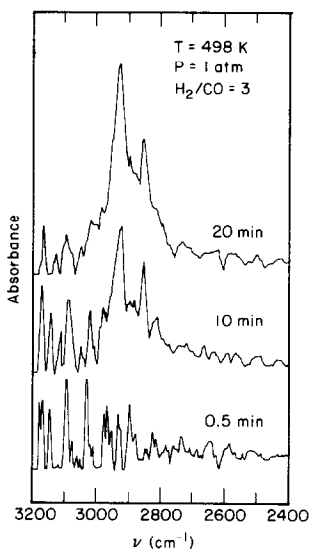


FIG. 7. Effects of reaction duration on the intensities of bands appearing between 2400 and 3200 cm^{-1} : $\text{H}_2/\text{CO} = 3$; $P = 1$ atm; $T = 498$ K.

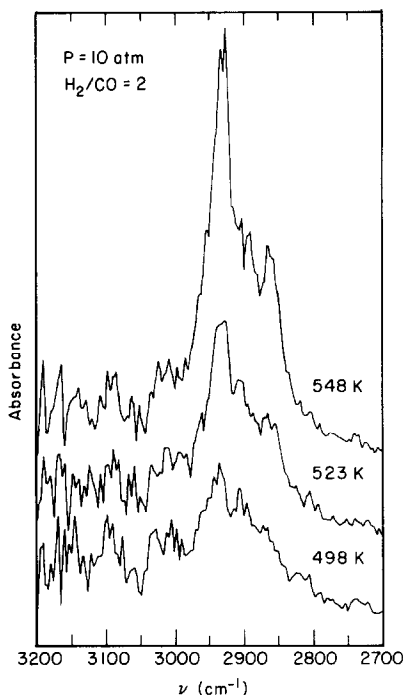


FIG. 8. Effects of temperature on the intensities of bands appearing between 2700 and 3200 cm^{-1} : $\text{H}_2/\text{CO} = 2$; $P = 10$ atm; observation time = 10 min.

and H_2/CO ratios exhibit the same set of bands observed in Fig. 7. By way of illustration, three spectra are shown in Fig. 8, taken after 10 min of reaction at temperatures of 498, 523, and 548 K; a pressure of 10 atm; and a H_2/CO ratio of 2. It is seen that the positions of the three bands remain fixed and are insensitive to changes in the reaction conditions. The increase in band intensities with increasing temperature can be associated with the more rapid rate of accumulation of species absorbing infrared radiation in this portion of the spectrum.

The stability of the bands in Figs. 7 and 8 were examined by treating the catalyst in various gas mixtures following reaction. Purging the reactor with He or a CO/He mixture at reaction temperature had no effect on the band intensities. The bands were rapidly attenuated, though, when a H_2/He mixture was introduced into the reactor. The rate of attenuation was found

to increase with increasing catalyst temperature and H_2 partial pressure.

Efforts were also made to determine whether the features appearing in Figs. 7 and 8 might be associated with reactions occurring on the alumina support. Passage of H_2/CO mixtures over an alumina disk failed to produce any bands over the temperature interval of 498 to 548 K. Weak bands were observed, though, when an alumina disk was placed in a cell immediately downstream of the cell containing the catalyst disk. Since the positions of the bands were identical to those observed in Figs. 7 and 8, these bands most likely arise from the adsorption of hydrocarbon products on the alumina disk.

The positions of the three bands found here are virtually identical to those which have been reported by Dalla Betta and Shelef (1), Ekerdt and Bell (2, 3), and King (4, 5) in studies of CO hydrogenation over alumina- and silica-supported Ru catalysts. The bands at 2930 and 2861 cm^{-1} can be assigned to the asymmetric and symmetric stretching of CH_2 groups present in saturated compounds, and the shoulder at 2960 cm^{-1} can be assigned to a methyl group (9). It is significant to note that in contrast to the work carried out by King (4, 5) with a Ru/Al_2O_3 catalyst, the position of the bands did not shift upscale with increasing reaction temperature and no hydrocarbon structures were formed by the interaction of CO and H_2 over alumina devoid of Ru.

On the basis of infrared spectra taken during CO hydrogenation over a Ru/Al_2O_3 catalyst, Dalla Betta and Shelef (1) concluded that the hydrocarbon bands observed could be ascribed to reaction products accumulated on the alumina support. The results of the present study also agree with this interpretation. The monotonic growth of the hydrocarbon bands beyond the point at which steady-state reaction has been attained, and the absence of any influence of the hydrocarbon band growth on the position or intensity of the CO band indicate that the hydrocarbon species are

unlikely to be on the Ru surface. Adsorption on the support is indicated by the observation of hydrocarbon bands on an alumina disk placed downstream of a catalyst disk and the report of similar bands when ethylene is adsorbed on η -alumina (32). Since α -olefins are the dominant C_{2+} hydrocarbons formed under the reaction conditions chosen for this study (6), it is reasonable to expect that the structures observed in the infrared spectra arise from the adsorption of these products at acid sites on the catalyst support. The carbonium ion thus formed would be stable in the absence of significant atomic hydrogen on the support surface. Since the surface of Ru is virtually saturated with CO under reaction conditions, little hydrogen spillover to the support would be expected. However, upon elimination of CO from the gas stream, the metal surface rapidly clears of adsorbed CO, and hydrogen can now adsorb freely. Spillover of hydrogen from the Ru to the alumina would then provide a source of atoms for removal of the adsorbed hydrocarbons.

CONCLUSIONS

The results of *in situ* infrared spectroscopy presented here demonstrate that the surface of a Ru/Al_2O_3 catalyst is covered primarily by linearly adsorbed CO. The coverage by this species depends on the catalyst temperature and the CO partial pressure, and is found to obey a Langmuir isotherm, characterized by an equilibrium constant of $K_{CO} = 1.1 \times 10^{-19} \exp(25,000/RT)$ (atm^{-1}). Moderate concentrations of diadsorbed CO (e.g., $Ru(CO)_2$) and small concentrations of μ -bridge-adsorbed CO (e.g., $Ru-CO-Ru$) were observed in addition to the linearly adsorbed form. The first of these species appears to be associated with either individual Ru atoms or small Ru clusters, which interact strongly with the alumina support. In contrast to the linearly adsorbed form of CO, diadsorbed CO does not react with H_2 at

temperatures below 548° K, and hence does not appear to participate in CO hydrogenation. The μ -bridged form of CO may occur in one of two possible forms. The first would be between a pair of Ru atoms, such that one atom bonds to the carbon end and the other Ru atom bonds to the oxygen end of the molecule. The second possibility is that the CO is attached through its carbon end to a Ru site and that the oxygen end interacts with a Lewis acid site on the support. Unfortunately, the amount of μ -bridge-adsorbed CO detected is too small to make any definitive conclusions regarding its role in CO hydrogenation.

Bands associated with adsorbed hydrocarbon, formate, and carbonate structures were also observed. The behavior of the hydrocarbon bands during and after reaction suggest that these structures are formed by the adsorption of olefinic hydrocarbons on the support. On the other hand, it appears that the formate and carbonate structures are formed on the surface of the alumina support via reactions of CO and H₂.

ACKNOWLEDGMENT

This work was supported by the Division of Chemical Sciences, Office of Basic Energy Sciences, U.S. Department of Energy under Contract W-7405-ENG-48.

REFERENCES

1. Dalla Betta, R. A., and Shelef, M., *J. Catal.* **48**, 111 (1977).
2. Ekerdt, J. G., and Bell, A. T., *Amer. Chem. Soc. Div. Pet. Chem. Prepr.* **23**, 475 (1978).
3. Ekerdt, J. G., and Bell, A. T., *J. Catal.* **58**, 170 (1979).
4. King, D. L., *Amer. Chem. Soc. Div. Pet. Chem. Prepr.* **23**, 482 (1978).
5. King, D. L., *J. Catal.* **61**, 77 (1980).
6. Kellner, C. S., and Bell, A. T., *J. Catal.* **71**, 288 (1981).
7. Kuznetsov, V. L., Bell, A. T., and Yermakov, Yu. I., *J. Catal.* **65**, 374 (1980).
8. Hicks, R. F., Kellner, C. S., Savatsky, B. J., Hecker, W., and Bell, A. T., *J. Catal.* **71**, 216 (1981).
9. Tripathi, S. C., Srivastava, S. C., Mani, R. P., and Shrimal, A. K., *Inorg. Chim. Acta* **15**, 249 (1975).
10. Thomas, G. E., and Weinberg, W. H., *J. Chem. Phys.* **70**, 1437 (1979).
11. Pfnür, H., Menzel, D., Hoffmann, F. M., Ortega, A., and Bradshaw, A. M., *Surface Sci.* **93**, 431 (1980).
12. Madey, T. E., and Menzel, D., *Japan. J. Appl. Phys. Suppl.* **2(2)**, 229 (1974).
13. Feulner, P., Engelhardt, H. A., and Menzel, D., *Appl. Phys.* **15**, 355 (1978).
14. Williams, E., and Weinberg, W. H., *Surface Sci.* **82**, 93 (1979).
15. Madey, T. E., *Surface Sci.* **79**, 575 (1979).
16. Rabo, J. A., Risch, A. P., and Poutsma, M. L., *J. Catal.* **53**, 295 (1978).
17. Ku, R., Gjostein, N. A., and Bonzel, H. P., *Surface Sci.* **64**, 465 (1977).
18. Fuggle, J. C., Umbach, E., Feulner, P., and Menzel, D., *Surface Sci.* **64**, 69 (1977).
19. Reed, P. D., Comrie, C. M., and Lambert, R. M., *Surface Sci.* **59**, 33 (1976).
20. Goodman, D. W., Madey, T. E., Ono, M., and Yates, J. T., Jr., *J. Catal.* **50**, 279 (1977).
21. Pfnür, H., Feulner, P., Engelhardt, H. A., and Menzel, D., *Chem. Phys. Lett.* **59**, 481 (1978).
22. Low, G. G., and Bell, A. T., *J. Catal.* **57**, 397 (1979).
23. Kettle, S. F. A., and Paul, I., *Adv. Organomet. Chem.* **10**, 199 (1972).
24. Dalton, J., Paul, I., and Stone, F. G. A., *J. Chem. Soc. A*, 2744 (1969).
25. Yates, J. T., Duncan, T. M., Worley, S. D., and Vaughn, R. W., *J. Chem. Phys.* **70**, 1219 (1979).
26. Dahl, L. F., Martell, C., and Wampler, D. L., *J. Amer. Chem. Soc.* **83**, 1761 (1961).
27. Kellner, C. S., and Bell, A. T., submitted for publication.
28. Colton, R., Commons, C. J., and Haskins, B. F., *J. Chem. Soc. Chem. Commun.*, 363 (1975).
29. Herrmann, W. A., Ziegler, M. L., Weidenhammer, K., and Biersack, H., *Angew. Chem. Int. Ed. Engl.* **18**, 960 (1979).
30. Kristoff, J. S., and Shiver, D. F., *Inorg. Chem.* **13**, 499 (1974).
31. Cant, N., and Bell, A. T., *J. Catal.*, in press.
32. Lucchesi, P. J., Carter, J. L., and Yates, D. J. C., *J. Phys. Chem.* **66**, 1451 (1962).